Flux qubits with neutral currents in optical lattices

Luigi Amico
CNR-MATIS-IMM & Dipartimento di Fisica e Astronomia, Via S. Sofia 64, 95127 Catania, Italy and Centre for Quantum Technologies, National University of Singapore, 3 Science Drive 2, Singapore 117543

Davit Aghamalyan
Centre for Quantum Technologies, National University of Singapore, 3 Science Drive 2, Singapore 117543

H. Crepaz, F. Auksztol, R. Dumke
Centre for Quantum Technologies, National University of Singapore, 3 Science Drive 2, Singapore 117543 and Division of Physics and Applied Physics, Nanyang Technological University, 21 Nanyang Link, Singapore 637371

L.-C. Kwek
Centre for Quantum Technologies, National University of Singapore, 3 Science Drive 2, Singapore 117543 and National Institute of Education and Institute of Advanced Studies, Nanyang Technological University, 1 Nanyang Walk, Singapore 637616

(Dated: April 18, 2013)

We study an experimentally feasible qubit system employing neutral currents. Our system is based on bosonic cold atoms trapped in ring-shaped optical lattice potentials. The lattice makes the system strictly one dimensional and it provides the infrastructure to realize a tunable ring-ring interaction. By breaking the Galilean invariance we demonstrate how atomic currents through the lattice provide a realization of a qubit. We break the Galilean invariance either by artificially creating a phase slip in a single ring, or by considering two homogeneous ring lattices, coupled by tunneling interaction. The Hamiltonian of the system effectively leads to a washboard potential in the phase representation, tilted by the applied 'flux'. The single qubit infrastructure is experimentally investigated with tailored optical potentials. An experimentally feasible scheme of the two-ring-qubit is discussed. In this case, the dynamics is demonstrated to show macroscopic quantum self trapping. Time-of-flight expansion maps the pattern of atomic currents into detectable atomic density distributions. Based on our analysis, we provide viable protocols to initialize, address, and read-out the qubit.

arXiv:1304.4615v1 [quant-ph] 16 Apr 2013

A qubit is a two state quantum system that can be manipulated coherently despite the environment, coupled to its neighbors, and measured. All proposed experimental implementations present qubit specific advantages and difficulties. These systems include ion traps[1], NMR[2], Josephson junctions[3], quantum dots[4] and cold atoms[5, 6]. In particular cold atoms and solid state Josephson junctions implementations have complementary characteristics. In neutral cold atoms proposals the qubit is encoded into well isolated internal atomic states. This allows long coherence times, precise state readout and in principle scalable quantum registers. However individual qubit (atom) addressing is a delicate point for optical lattice architectures[7]. Qubits based on Josephson junctions implement the two level system either using charge or by clockwise-anticlockwise superconducting currents. Such devices allow fast gate operations and make use of the precision reached by lithography techniques for circuit design [8]. The decoherence, however, is fast in these systems and it is experimentally challenging to reduce it. For charge qubits the main problem arises from dephasing due to background charges in the substrate[9]. Flux qubits are insensitive to the latter decoherence source, but are influenced by magnetic flux fluctuations due to impaired spins proximal to the device[10].

Here we aim at bringing together the advantages characterizing Josephson junctions and cold atoms. The basic idea is to use the neutral currents flowing through ring shaped optical lattices to realize the cold atoms analog of flux qubits[11]. Persistent currents in optical ring lattices are experimentally generated in different ways: by rotating the condensates[12, 13], by exploiting dark-states[14–16], or by implementing the phase slips as a Berry phase[11, 17]. Superpositions of persistent currents have been thoroughly investigated in a series of papers by Rey *et. al.* In the case of homogeneous rings the superposition state can in principle occur but with important restrictions on the density of superfluid and strength of the interaction; further, the visibility of the two states vanishes in the thermodynamic limit[18, 19]. Some of these limitations can be overcome by breaking the Galilean invariance of the system[20, 21].

In this paper we demonstrate how persistent currents flowing in a ring shaped optical lattice[11] can provide a physical implementation of a qubit. The lattice potential plays an important role in our approach because it provides the confinement of the atoms in a strictly one dimensional ring. Further it provides the means for precise control of the confinement and facilitates the qubit-qubit interaction. In our system we break the Galieian invariance. For a single ring this is realized by creating a localized 'defect' barrier along a homogeneous lattice[22]. Furthermore we prove that a qubit can be achieved with two homogeneous interacting rings arranged vertically on top of each other. In such a system the Galilean invariance is broken along the direction transverse to the two rings. For this scheme we analyze the real time dynamics and time-of-

flight density distributions.

Breaking the Galilean invariance on the single ring– We consider bosonic atoms loaded in a ring-shaped potential with identical wells, but with a dimple located at the site $N-1$ (see Fig.1), and pierced by a 'magnetic flux' Φ. The system is described by the Bose Hubbard Hamiltonian

$$H_{BH} = \frac{U}{2}\sum_{i=0}^{N-1} n_i(n_i-1) - \sum_{i=0}^{N-1} t_i(e^{i\Phi/N}a_i^\dagger a_{i+1} + h.c.) \quad (1)$$

where a_i's are bosonic operators for atoms trapped in the the ring and $n_i \doteq a_i^\dagger a_i$. The parameters t_i describe the tunneling between the wells along the ring. Since the wells are all identical but one, $t_i = t, \forall i = 0 \dots N-2$ and $t_{N-1} = t'$. Finally, U describes the s-wave scattering interaction [26]. The 'magnetic flux' is $\Phi = \int_{x_i}^{x_{i+1}} \boldsymbol{A(z)}dz$, where $\boldsymbol{A(z)}$ is the effective vector potential. The effect of the dimple is to induce a phase slip at the site $N-1$. We assume that the density of superfluid is large enough to neglect the fluctuation of the number of atoms in each well. In this regime we can assume that the system dynamics is characterized by the phases of the superfluid order parameter ϕ_i's, described by the quantum phase model [27] with Josephson coupling $J_i = \langle n\rangle t_i$ ($\langle n\rangle$ is the average number of bosons in each well). The magnetic flux Φ can be gauged away everywhere but at the site $(N-1)$-th [28–30]. Accordingly the phase difference along nearest neighbor sites can be considered small in the 'bulk' and the harmonic approximation can be applied. The partition function can be written as a path integral: $Z = \int \mathcal{D}[\phi]e^{-S[\phi]}$, where the $S[\phi]$ is the Euclidean action. Adapting from the approach pursued by Rastelli et al. [33], all the phases ϕ_i except $\theta \doteq \phi_{N-1} - \phi_0$ can be integrated out (the integrals are gaussian). The effective action reads

$$S_{eff} = \int_0^\beta d\tau\left[\frac{1}{2U}\dot{\theta}^2 + \frac{J}{2(N-1)}(\theta-\Phi)^2 - J'\cos(\theta)\right] - \frac{J}{2U(N-1)}\int d\tau d\tau'\theta(\tau)G(\tau-\tau')\theta(\tau') \quad (2)$$

with the potential $U(\theta) \doteq \frac{J}{N-1}(\theta-\Phi)^2 - J'\cos(\theta)$. For large $(N-1)J'/J$ and moderate N, $U(\theta)$ defines a two-level system. The degeneracy point is $\Phi = \pi$: The two states are provided by the symmetric and antisymmetric combination of counter-circulating currents corresponding to the two minima of $U(\theta)$. We observe that breaking the Galilean invariance of the system provides an independent parameter J' facilitating the control of the potential landscape. The interaction between θ and the (harmonic) bulk degrees of freedom provides the non local term with $G(\tau) = \sum_{l=0}^{\infty} Y(\omega_l)e^{i\omega_l\tau}$, ω_l being Matsubara frequencies and $Y(\omega_l) = \omega_l^2 \sum_{k=1}^{(N-2)/2} \frac{1+\cos[2\pi k/(N-1)]}{2JU(1-\cos[2\pi k/(N-1)]) + \omega_l^2}$. The external bath vanishes in the thermodynamic limit and the effective action reduces to the Caldeira-Leggett one [33, 34]. Finally it is worth noting that the case of a single junction needs a specific approach but it can be demonstrated consistent with Eq.(2)[35] .

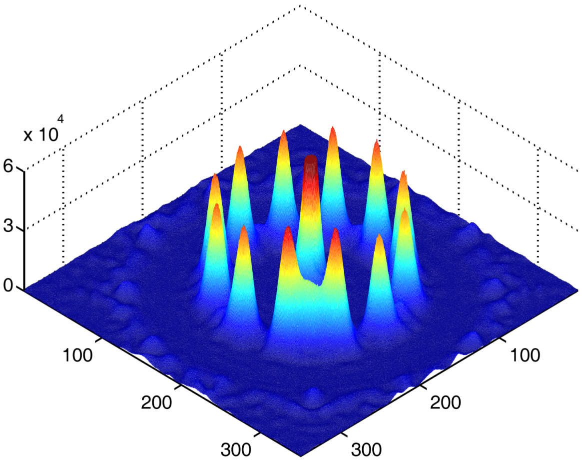

FIG. 1. Realization of a ring-lattice potential with an adjustable weak link. We create the optical potential with a spatial light modulator (SLM) which imprints a controlled phase onto a collimated laser beam. The figure above shows a measured intensity distribution (arb. units) with horizontal axes units in μm. The center peak is the residual zero-order diffraction. The structure is scalable and a lower limit is imposed by the optical wavelength. The ring lattice resembles the single qubit potential as discussed in Eq.(2). Calculation of the SLM phase pattern (kinoform) has been carried out using an improved version of the Mixed-Region-Amplitude-Freedom (MRAF) algorithm[22, 23] with angular spectrum propagator[24]. This allows us to calculate numerically the wavefront propagation without resorting to paraxial approximation. For calculation of the holograms an undistorted Gaussian wavefront as input intensity distribution for the kinoform has been assumed. A region outside the desired ring lattice pattern is dedicated to collect unwanted light contributions resulting from the MRAF algorithm's iterative optimization process.

Breaking the Galilean invariance with two homogenous coupled rings–We consider bosonic atoms loaded in two identical rings Fig.2. The system is described by Bose-Hubbard ladder: $H = H_{BH}^{(a)} + H_{BH}^{(b)} + H_{int}$, where $H_{BH}^{(a,b)}$ are the Hamiltonians as in Eq.(1) describing the bosons in the rings a and b respectively. The interaction is:

$$H_{int} = -g\sum_{i=1}^{N}(a_i^\dagger b_i + b_i^\dagger a_i). \quad (3)$$

We observe that along each ring the phase slips imply twisted boundary conditions and therefore they can be localized to a specific site, say the $N-1$-th. Following a similar procedure as employed above, the effective action reads

$$S_{eff} = \int_0^\beta d\tau\left[\frac{1}{2U}\sum_{\alpha=a,b}\dot{\theta_\alpha}^2 + U(\theta_a,\theta_b)\right] - \frac{J}{2U(N-1)}\sum_{\alpha=a,b}\int d\tau d\tau'\theta_\alpha(\tau)G_\alpha(\tau-\tau')\theta_\alpha(\tau') \quad (4)$$

where each $G_\alpha(\tau)$ is given by the expression found above for the case of a single ring. In this case the phase dynamics is

provided by the potential

$$U(\theta_a,\theta_b) \doteq \sum_{\alpha=a,b}\left[\frac{J}{2(N-1)}(\theta_\alpha-\Phi_\alpha)^2 - J\cos(\theta_\alpha)\right] \\ -\tilde{J}\cos[\theta_a-\theta_b-\frac{N-2}{N}(\Phi_a-\Phi_b)]\,. \quad (5)$$

with $\tilde{J} = \langle n\rangle g$. We observe that, for large N, the potential $U(\theta_a,\theta_b)$ provides that effective phase dynamics of Josephson junctions flux qubits realized by Mooji *et al.* (large N's corresponds to large geometrical inductance of flux qubit devices) [32]. In there, the landscape was thoroughly analyzed. The qubit is made with superpositions of the two states $|\theta_1\rangle$ and $|\theta_2\rangle$ corresponding to the minima of $U(\theta_a,\theta_b)$. The degeneracy point is achieved by $\Phi_b-\Phi_a=\pi$. We comment that the ratio $\tilde{J}/J$ controls the relative size of the energy barriers between minima intra- and minima inter-'unit cells' of the (θ_a,θ_b) phase space, and therefore is important for designing the qubit. In our system $\tilde{J}/J$ can be fine tuned with the scheme shown in Fig.2.

We now study the dynamics of two homogeneous rings coupled by tunneling. We will show that the density of the condensate in the two rings can display characteristic oscillations in time. We make use of the mean field approximation to analyze the (real time) dynamics of the Bose-Hubbard ladder Eqs.(1), (3) (assuming that each ring is in a deep superfluid phase). Accordingly Gross-Pitaevskii equations are found for the variables $\varphi_{a,i}(s)=\langle a_i(s)\rangle$ and $\varphi_{b,i}(s)=\langle b_i(s)\rangle$. Assuming that $\theta_\alpha \doteq \varphi_{\alpha,i+1}-\varphi_{\alpha,i}$ in each ring is site-independent, we obtain

$$\frac{\partial z}{\partial\tilde{s}} = -\sqrt{1-z^2}\sin\Theta \\ \frac{\partial\Theta}{\partial\tilde{s}} = \Delta+\lambda\rho z+\frac{z}{\sqrt{1-z^2}}\cos\Theta \quad (6)$$

where $z=(N_b-N_a)/(N_a+N_b)$ is the normalized imbalance between the populations N_a and N_b of the two rings, $\Theta=\theta_a-\theta_b$ and $\tilde{s}\doteq 2gs$ ($\hbar=1$). The parameters are $\Delta=\left[\mu_a-\mu_b+t(\cos\frac{\Phi_a}{N}-\cos\frac{\Phi_b}{N})\right]/g$, $\lambda=U/(2g)$, and $\rho=(N_a+N_b)/N$ is the total bosonic density (we included the chemical potential μ_α). Eqs.(6) can be solved analytically in terms of elliptic functions[36]. Accordingly, the dynamics displays distinct regimes (oscillating or exponential) as function of the elliptic modulus k, depending in turn on Δ, λ, and on the initial population imbalance $z(0)\doteq z_0$. Here we consider the dynamics at $\lambda\rho\ll\Delta$, *i.e.* small U/g (the analysis of the solutions of the Eqs.(6) in different regimes will be presented elsewhere). The results are summarized in Fig.3. We comment that, comparing with $\Delta=0$, the oscillations do not average to zero (therefore yielding a macroscopic quantum self trapping phenomenon [36]) and they are faster.

The pattern of the circulating currents along the two coupled rings can be read out through the analysis of the time-of-flight density. As customarily, the spatial density distribution in the far field corresponds to the distribution in the momentum space at the time when the confinement potential is turned off:

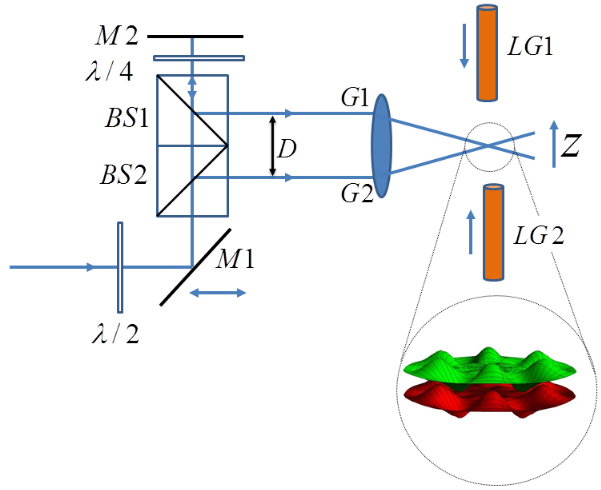

FIG. 2. The proposed setup for the ring-ring coupling. Two parallel gaussian laser beams (G1,G2) with wavelength λ_1 are produced by a combination of two polarizing beamsplitter (BS1, BS2). The beam separation D can be controlled by moving mirror M_1. The beams pass through a lens with focal length f and interfere to form a lattice in z-direction. The distance between the lattice planes is a function of $1/D$ [31]. The resulting one dimensional lattice is combined with two counter propagating Laguerre-Gaussian laser beams (LG1, LG2) of amplitude E_0 and wavelength λ_2. To avoid interference between the lattice in z-direction and the Laguerre-Gaussian beams, the wavelength difference between λ_1 and λ_2 should be large, typically a few nm. The inset shows the ring lattice potentials separated by $d=\lambda_1 f/D$: $V_{latt}=4E_0^2(f_{pl}^2\cos{(k_{LG}z)}^2+\cos{(k_G z)}^2+2f_{pl}\cos{(k_{LG}z)}\cos{(k_G z)}\cos{(\phi l)})$, where f_{pl} are related to Laguerre functions [11]. In the figure $l=6$ and $p=0$. The ring-ring distance is adjustable by varying the distance D. The WKB estimate of the tunneling rate gives $g\simeq\exp{(-4E_0^2 f_l\lambda f/D)}$. Such a system provides an effective two level system that can be exploited as a qubit (see text).

$$\rho(\mathbf{k}) = \frac{|w(k_x,k_y,k_z)|^2}{N}\sum_{i=0}^{N-1}\sum_{j=0}^{N-1}\sum_{q\in\{2\pi n/N\}} \quad (7) \\ \Big[\cos{[\mathbf{k}_\parallel\cdot\mathbf{x}_\parallel+(q+\frac{\Phi_a}{N})(\phi_i-\phi_j)]}\langle a_q^\dagger a_q\rangle+ \\ \cos{[\mathbf{k}_\parallel\cdot\mathbf{x}_\parallel+(q+\frac{\Phi_b}{N})(\phi_i-\phi_j)]}\langle b_q^\dagger b_q\rangle+ \\ 2\cos{[\mathbf{k}_\parallel\cdot\mathbf{x}_\parallel+k_z D+(q+\frac{\Phi_a}{N})\phi_i-(q+\frac{\Phi_b}{N})\phi_j)]}\langle a_q^\dagger b_q\rangle\Big]$$

where $w(k_x,k_y,k_z)$ are Wannier functions (that we considered identical for the two rings), $\mathbf{k}_\parallel\cdot\mathbf{x}_\parallel\doteq k_x(x_i-x_j)+k_y(y_i-y_j)$, $x_i=\cos\phi_i$, $y_i=\sin\phi_i$ fix the positions of the ring wells in the three dimensional space, $\phi_i=2\pi i/N$ being lattice sites along the rings. The density Eq.(8) is displayed in Fig.4

Conclusions– We discussed a construction of flux qubits with atomic neutral currents flowing in ring-shaped optical

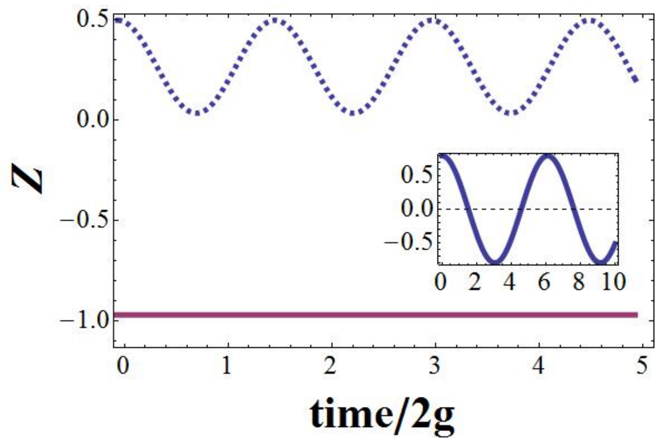

FIG. 3. The population imbalance in two coupled rings. We focused on the case $\Delta \gg \lambda\rho$. For moderate z_0, oscillations are obtained, with $\omega = 2g\left\{\sqrt{1+\Delta^2} + \lambda\rho(z_0\Delta - \sqrt{1-z_0^2})(2\Delta^2-1)/[2(1+\Delta^2)^{3/2}]\right\}$ corresponding to macroscopic quantum self trapping. The dynamics can be visualized with the help of the mechanical system provided by a rotator of length $\sqrt{1-z(s)^2}$, driven by the external force Δ. The constant solution $z(t) = const$ corresponds to vanishing pendulum length. For $\Delta = 0$ (inset), the dynamics is characterized by Rabi oscillation with $\omega_0 \doteq 2g(1+\lambda\rho\sqrt{1-z_0}/2) < \omega$. Here $\lambda\rho = 0.1$ and $\Delta = 4$ implying that $\omega \approx 4\omega_0$.

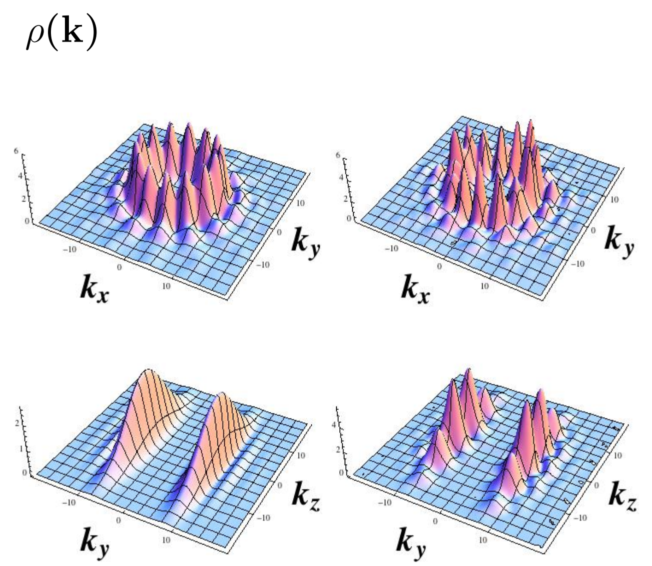

FIG. 4. The time of flight expansion for the two-coupled-rings-qubit. Left panel: vanishing inter-ring tunneling rate $g/t = 0$. Right panel: $g/t = 0.9$. In the (k_x, k_y) plane the interference fringes with the ring symmetry are due to the momenta of the quantum degenerate gas; the inter-ring tunneling suppresses the interference fringes. In the (k_y, k_z) plane g, induces structured interference fringes. The Eq. (8) is calculated for the Bose-Hubbard ladder with 'fluxes' Φ_a and Φ_b, with $U = 0$, and at quantum degeneracy. In the plots: $\Phi_a = 80, \Phi_b = 70$, $T = 0.05k_B$ and $N = 14$ with filling fractions of 10 bosons per site.

lattice potentials. Persistent currents had been experimentally observed [37] in a narrow toroidal trap with a weak link. The effective action of the system studied in [38] can provide a two level system. In contrast with [37, 38], we emphasize how we make explicit use of the lattice in our construction, both to confine the particles in the rings and to drive the ring-ring interaction. The qubits are realized by breaking the Galilean invariance of the system either by adding an additional barrier along a single ring lattice Eqs.(2), or by tunnel coupling of two homogeneous rings, Eq.(5). The latter is proposed to be realized with the scheme in Fig.2. At the degeneracy point basis, the effective Hamiltonians (2) and (5) lead to one and two qubit operations (see [39]).
Our work provides a feasible route to the implementation of a functional flux qubit based on persistent atomic currents. The initialization of our qubit can be accomplished, for example, imparting rotation by exploiting light induced torque from Laguerre-Gauss (LG) beams carrying optical angular momentum. A two-photon Raman transition between internal atomic states can then be used to transfer coherently $\hbar$ orbital angular momentum to the atoms. With this method, transfer efficiencies of 90% to the rotating state had been demonstrated [37, 40]. Owing to the coherent nature of the Raman process, superpositions of different angular momentum states can be prepared [41, 42]. Measurements of the decay dynamics of a rotating condensate in an optical ring trap showed remarkable long lifetimes of the quantized flow states on the order of tens of seconds even for high angular momentum (l=10)[41]. Condensate fragmentation and collective excitations which would destroy the quantum state had not been observed. To allow controlled tunneling between neighboring lattice stacks the distance between the ring potentials needs to be adjustable in the optical wavelength regime (the schematics in Fig.2 can be employed). Small distances allow high tunneling rates, a necessity for fast gate operations. This makes it however less efficient to read out and address individual stack sites. Increasing the lattice stack separation after the tunneling interaction has occurred well above the diffraction limit while keeping the atoms confined, optical detection and addressing of individual rings becomes possible.

Read out of the angular momentum states can be accomplished experimentally with interference of different flow states (i.e. corresponding to a fragmented superfluid) which maps the phase winding into a density modulation that can be measured using time-of-flight imaging [41]. In the lower panel of Fig.4 it is shown that different flow states lead to characteristic density patterns in the far field.

We believe that our implementation combines the advantages of neutral cold atoms and solid state Josephson junction based flux qubits for applications in quantum simulation and computation. This promises to exploit the typically low decoherence rates of the cold atom systems, overcoming the single site addressing, and harness the full power of macroscopic quantum phenomena in topologically non trivial systems. The characteristic fluctuations in the magnetic fields affecting Josephson junction based flux qubits are expected to

be minimized employing neutral atoms as flux carriers.

Acknowledgments.— We are grateful to A. J. Leggett for his constant support since the early stages of this work and for a critical reading of the manuscript. We thank F. Cataliotti, R. Fazio, F. Hekking, F. Illuminati, and G. Rastelli for discussions, and B. DeMarco for providing the original MRAF algorithm.

[1] Blatt, R., and D. Wineland, Nature **453**, 1008 (2008).
[2] L.M. K. Vandersypen , M. Steffen, G. Breyta, C.S. Yannoni, M. H. Sherwood, and I.L. Chuang, Nature **414**, 883 (2001).
[3] J. Clarke and F.K. Wilhelm, Nature **453**, 1031 (2008).
[4] J. Petta, A. Johnson, J. Taylor, E. Laird, A. Yacoby, M. Lukin, C. Marcus, M. P. Hanson, and A. Gossard, Science **309**, 2180 (2005).
[5] I. Bloch, Nature **453**, 1016 (2008).
[6] M. Saffman, T. G. Walker, K. Molmer, Rev. Mod. Phys. **82**, 2313 (2010).
[7] J. F. Sherson, C. Weitenberg, M. Endres, M. Cheneau, I. Bloch, and S. Kuhr, Nature **467**, 68 (2010); C. Weitenberg, M. Endres, J.F. Sherson, M. Cheneau, P. Schauss, T. Fukuhara, I. Bloch, and S. Kuhr, Nature **471**, 319 (2011).
[8] E. Lucero, R. Barends, Y. Chen, J. Kelly, M. Mariantoni, A. Megrant, P. O'Malley, D. Sank, A. Vainsencher, J. Wenner, T. White, Y. Yin, A. N. Cleland, John M. Martinis Nature Physics **8**, 719 (2012).
[9] E. Paladino, L. Faoro, G. Falci, and R. Fazio, Phys.Rev. Lett. **88**, 228304 (2002).
[10] L. L. S. Tian, L. S. Levitov, C. H. van der Wal, J. E. Mooij, T. P. Orlando, S. Lloyd, C. J. P. M. Harmans, and J. J. Mazo, 2000, in *Quantum Mesoscopic Phenomena and Mesoscopic Devices in Microelectronics*, edited by I. Kulik, and R. Elliatioglu, (Kluwer Ac. Publ., Dordrecht); cond-mat/9910062.
[11] L. Amico, A. Osterloh, and F. Cataliotti, Phys. Rev. Lett. **95**, 063201 (2005).
[12] K. W. Madison, F. Chevy, W. Wohlleben, and J. Dalibard,Phys. Rev. Lett. **84**, 806 (2000).
[13] J. R. Abo-Shaeer, C. Raman, J. M. Vogels, and W. Ketterle, Science **292**, 476 (2001).
[14] Y.-J. Lin, R. L. Compton, K. Jimnez-Garca, J. V. Porto, and I. B. Spielman, Nature **462**, 628 (2009).
[15] Y. - J. Lin, R. L. Compton, K. Jimnez-Garcia, W. D. Phillips, J. V. Porto, and I. B. Spielman , Nature Physics **7**, 531 (2011).
[16] N. R. Cooper and Z. Hadzibabic, Phys. Rev. Lett. **104**, 030401 (2010).
[17] A. E. Leanhardt *et al*, Phys. Rev. Lett. **89**, 1905403 (2002).
[18] D. Hallwood, K. Burnett, and J. Dunningham, New J. Phys. **8**, 180 (2006).
[19] A. Nunnenkamp, A. M. Rey, and K. Burnett, Phys. Rev. A **77**, 023622 (2008); A. Nunnenkamp and A. M. Rey, J. Mod. Opt. **55**, 3339 (2008).
[20] D. Hallwood, T. Ernst, and J. Brand, Phys. Rev. A **82**, 063623 (2010).
[21] A. Nunnenkamp, A. M. Rey, and K. Burnett, Phys. Rev. A **84**, 053604 (2011).
[22] M. Pasienski and B. DeMarco, Optics Express, **16**, 2176 (2008).
[23] A. L. Gaunt and Z. Hadzibabic, Nature Scientific Rep. **2**, 721 (2012).
[24] J. W. Goodman, *Introduction to Fourier Optics*, 3rd ed. (Roberts & Company Publishers, 2005)
[25] S. Franke-Arnold, J. Leach, M. J. Padgett, V. E. Lembessis, D. Ellinas, A. J. Wright, J. M. Girkin, P. Ohberg, and A. S. Arnold Optics Express, **15**, 8619 (2007).
[26] D. Jaksch, C. Bruder, J.I. Cirac, C.W. Gardiner, and P. Zoller, Phys. Rev. Lett. **81**, 3108 (1998).
[27] R. Fazio and H. van der Zant, Phys. Rep. **355 (4)**, 235 (2001).
[28] B. S. Shastry and B. Sutherland, Phys. Rev. Lett. **65**, 243 (1990).
[29] H. J. Schulz and B. S. Shastry, Phys. Rev. Lett. **80**, 1924 (1998).
[30] A. Osterloh, L. Amico, U. Eckern, Nucl. Phys. B **588**, 531 (2000).
[31] T. C. Li, H. Kelkar, D. Medellin, and M.G.Raizen, Optics Express,Vol. **16**,No.8,5468 (2008).
[32] J. E. Mooij, T. P. Orlando, L. Levitov, L. Tian, C. H. van der Wal, and S. Lloyd, Science **285**, 1036 (1999).
[33] G. Rastelli, I. M. Pop, W. Guichard, F. W. J. Hekking, arXiv:1201.0539.
[34] A. Caldeira and A. J. Leggett, Phys. Rev. Lett. **46**, 211 (1981).
[35] U. Eckern, G. Schön and V. Ambegaokar, Phys. Rev. A **30**, 6419 (1984).
[36] S. Raghavan, A. Smerzi, S. Fantoni and S. R. Shenoy, Phys. Rev. A **59**, 620633 (1999)
[37] C. Ryu, M. F. Andersen, P. Clad, Vasant Natarajan, K. Helmerson, and W. D. Phillips Phys. Rev. Lett. **99**, 260401 (2007); A. Ramanathan, K. C. Wright, S. R. Muniz, M. Zelan, W. T. Hill III, C. J. Lobb, K. Helmerson, W. D. Phillips, G. K. Campbell Phys. Rev. Lett. **106**, 130401 (2011).
[38] D. Solenov and D. Mozyrsky, Phys. Rev. Lett. **104**, 150405 (2010); J. Comput. Theor. Nanosci. **8**, 481 (2011); Phys. Rev. A **82**, 061601(R) (2010).
[39] Y. Makhlin, G. Schön, and A. Shnirman, Rev. Mod. Phys. **73**, 357 (2001).
[40] J. F. S. Brachmann, W. S. Bakr, J. Gillen, A. Peng, M. Greiner, Optics Express, **19**, 12984-12991 (2011).
[41] S. Moulder, S. Beattie, R. P. Smith, N. Tammuz, Z. Hadzibabic, Phys. Rev. A **86**, 013629 (2012).
[42] K. T. Kapale, J. P. Dowling, Phys. Rev. Lett. **95**, 173601 (2005); S. Thanvanthri, K. T. Kapale, J. P. Dowling, Phys. Rev. A **77**, 053825 (2008).